Photodissociation of Dimethylmercury in Argon Matrixes by 193 and 248 nm Laser Irradiation

Claudine Crépin,*,† Nicole Legay-Sommaire,† John G. McCaffrey,‡ and André Tramer†

Department of Chemistry, National University of Ireland at Maynooth, Maynooth, Co. Kildare, Ireland, and
Laboratoire de Photophysique Moléculaire du CNRS, Bâtiment 210, Université de Paris-Sud,
91405 Orsay Cedex, France

Received: January 16, 1998; In Final Form: March 16, 1998

The photodissociation of dimethylmercury, $Hg(CH_3)_2$, in dilute argon matrixes is induced efficiently by ArF (193 nm) and inefficiently by KrF (248 nm) laser irradiation. The reaction products are identified by their IR absorption and UV absorption and luminescence spectra. Upon ArF photolysis, ethane remaining in close proximity of a Hg atom ($Hg{\cdot}C_2H_6$) is the main reaction product. The $Hg{\cdot}C_2H_6$ complex is destroyed by KrF radiation with formation of $HHgC_2H_5$, which is photolyzed, giving HgH_2 and ethylene. Unidentified near UV emission bands recorded during irradiation are tentatively assigned to an unstable $Hg{\cdot}CH_3$ complex.

Introduction

The photodissociation of the dimethylmetals, $M(CH_3)_2$, has been studied in the gas phase, although the attention was focused on its cadmium and zinc analogues, $Cd(CH_3)_2$ and $Zn(CH_3)_2$, rather than on dimethylmercury, $Hg(CH_3)_2$. The absorption spectra of all three compounds in the 106−300 nm range are known.[1,2] In the spectral range relevant to the present work (190−250 nm), $Hg(CH_3)_2$ exhibits two absorption bands, the weak A ← X transition centered at 43 000 cm^{-1} and the stronger B ← X at 50 500 cm^{-1}. Their assignments to the valence[1] or Rydberg[2] transitions is controversial. Both bands exhibit a diffuse vibrational structure showing that the A and B states are not dissociative but strongly predissociated. The lifetime of the $Cd(CH_3)_2$ A-state, deduced from the bandwidths of its fluorescence excitation spectrum obtained in the supersonic expansion, is of the order of 50 fs.[3,4] The absorption spectra of $Hg(CH_3)_2$ in the gas, at room temperature,[1] suggest slightly longer lifetimes of the A- and especially of the B-state. Two dissociation channels[2,3,5,6] have been identified in the case of the one-photon excitation of the A and B states of $Cd(CH_3)_2$ and $Zn(CH_3)_2$ in the gas phase. These channels can be summarized as

$$M(CH_3)_2 \rightarrow MCH_3 + CH_3 \qquad (1)$$

or

$$M(CH_3)_2 \rightarrow M + 2CH_3 \qquad (2)$$

where M = Zn, Cd. For $Zn(CH_3)_2$, the first step produces the monomethyl radical in a vibrationally excited state; the second, unimolecular dissociation of the vibrationally "hot" methylzinc radical then produces methyl radical and atomic zinc. The first channel was not observed for $Hg(CH_3)_2$ in the gas phase, the weakly bound $HgCH_3$ radical[7] being probably unstable in the presence of collisions. It is noteworthy, however, that in the IR spectra of matrix isolated products of the gas-phase pyrolysis of $Hg(CH_3)_2$, Snelson[8] observed, beside the main products CH_3 and ethane, very weak lines assigned to $HgCH_3$.

On the other hand, upon the excitation of $Zn(CH_3)_2$ and $Cd(CH_3)_2$ in their B ← X transitions, by the 193 nm line of the ArF laser, atomic emission from the Zn and Cd $^3P_1$ states was observed.[3,4,6] Since the $M(CH_3)_2 + h\nu \rightarrow M^* + 2CH_3$ reaction, where $M^* = M\ ^3P_1$, requires more energy than that of a single 193 nm photon, this process must be due to the two-photon absorption involving the B-state as the intermediate level. This assignment was confirmed by the quadratic dependence of the intensity of the atomic fluorescence on the laser flux.[6] No systematic study of $Hg(CH_3)_2$ behavior upon 193 nm irradiation has been carried out, but the electronic emission induced in the gas phase by the ArF laser is mentioned by Baughcum and Leone.[9] Upon 248 nm excitation, these authors observed uniquely the $Hg(CH_3)_2 + h\nu \rightarrow Hg(^1S_0) + 2CH_3$ channel (infrared emission from vibrationally excited methyl radicals).

The UV absorption spectrum of matrix-isolated dimethylzinc has been observed with synchrotron radiation.[10a] A strong blue shift was observed on the B, A ← X transitions and no luminescence was recorded with excitation of either of these transitions. The experimental study of photochemistry of $Zn(CH_3)_2$ isolated in Ar matrixes has been achieved with ArF laser photolysis, and the products have been detected by FTIR absorption spectroscopy[10b] and UV luminescence. Two types of products were identified: ethane and CH_3 radical perturbed by the Zn atom. Secondary products C_2H_5ZnH and C_2H_4 were observed after prolonged photolysis.

Since the pioneering work of Gutowsky,[11] vibrational spectra of dimethylmetals were extensively studied in gas and liquid phase by infrared and Raman spectroscopy,[12,13] completed by the normal coordinate analysis[14] and ab initio calculations,[15] but there is only one, low-resolution study of the IR absorption of $Hg(CH_3)_2$ in argon matrixes.[16] The identification of vibrational modes is then completed in Ar and nitrogen matrixes in this work.

After a short survey of spectroscopic observations on $Hg(CH_3)_2$ isolated in matrixes, this article describes and analyses the data obtained on samples irradiated by an excimer laser,

---

† Université de Paris-Sud.

‡ National University of Ireland at Maynooth.

S1089-5639(98)00797-X CCC: $15.00

yielding information on the photodissociation processes occurring at low temperature in matrixes.

Experimental Section

For the UV experiments, thin $Hg(CH_3)_2$/Ar films were prepared by the condensation of gaseous $Hg(CH_3)_2/Ar \approx 1/2500$ or 1/1000 mixtures on a sapphire sample holder of a closed-cycle Air Products helium cryostat at 14 K. The previously prepared mixture flows through a needle valve regulating the deposition rate. The gases, Ar of 99.9999% purity from Messer France, dimethylmercury of 98% purity from Strem Chemicals, C_2H_6 (99.95%) and C_2H_4 (99.7%) from Messer France, C_2D_6 with 99% deuterium purity from Euriso-top, and C_2H_2 (99.6%) from Air Liquid, were used without further purification. Samples were deposited and spectra recorded at 12−14 K, and samples were not annealed in order to avoid formation of clusters.

The light source used for UV absorption spectra was a deuterium lamp. Emission and excitation spectra were recorded upon excitation by a frequency-doubled dye laser (Lambda Physik, model FL2002) with a 0.5 cm^{-1} line width, pumped by a XeCl excimer laser (Lambda Physik, model EMG102), using a 0.6 m Jobin-Yvon monochromator with a spectral resolution of ca. 10 cm^{-1} equipped with a RTCXP2020Q photomultiplier (PMT). The spectra of the prompt (Hg $^3P_1 \rightarrow {}^1S_0$) emission were obtained by sending the PMT signal through an EG&G 460 shaping amplifier to a LeCroy gated integrator (Evans card). Decay curves of the emission were obtained by sending the PMT signal directly to a 3400 LeCroy digital oscilloscope. Absorption and long-lived emission $^3P_0 \rightarrow {}^1S_0$ spectra were recorded by using the photon counting system (time-gated with respect to the laser pulse if needed) via a Labmaster card interfaced with a microcomputer. Decay curves were obtained on a 3521A LeCroy multichannel scaling module in the Camac crate.

Band positions are reproducible within an error of ± 20 cm^{-1}. Decay curves were always fitted to a single exponential function, despite a better fitting by double exponential functions. Deviations from an exponential decay are not reproducible and are probably due to different environments of the emitting center. We preferred, therefore, to estimate average decay rates despite a relatively large dispersion (5−10%) of the decay times.

The device used for IR measurements has been previously described.[17] It consists of a 4 L SMC liquid helium cryostat placed in the absorption chamber of a Bruker IFS 120 FTIR spectrometer. The cryostat is equipped with a CsBr sample holder which may be rotated between three positions perpendicular to the sample deposition tube, to the axis of the ArF/KrF laser beam, and to the optical axis of the spectrometer. The spectrometer was operated with a KBr beam splitter and a MCT detector. All the spectra were recorded at 12 K from the accumulation of 200 scans at an instrument resolution of 0.1 cm^{-1}. The concentration of dimethylmercury in the samples was between 2×10^{-3} and 2.5×10^{-4} and the thickness approximately 1 mm.

The photolysis laser used in both the UV luminescence and IR absorption work was an excimer laser (SOPRA or Lambda-Physics) working either on ArF (193 nm) or KrF (248 nm) emission. The intensity of the 3 Hz pulses, measured at the sample, was about 2 mJ/pulse for ArF and 6−10 mJ/pulse for KrF. Unless stated otherwise, the direct, unfocused output of the laser was used.

The effects of the ArF or KrF laser irradiation were followed with the two independent UV an IR setups described above by recording (i) the UV emission spectra observed during laser irradiation of the sample, (ii) UV and IR absorption spectra of samples irradiated for specified periods of time and with different laser intensities, and (iii) the spectra and decay times of the UV emission from irradiated samples upon excitation with a dye laser or strongly attenuated KrF and ArF lasers.

TABLE 1: $Hg(CH_3)_2$ Wavenumbers

	gas[12]	argon matrix	N_2 matrix
ν_1	2907		
ν_2	1198.2		
ν_3	518		522.9
ν_5	2905	2908	2907.5
			2911.3
			2913.4
		2916.6	2916.1
ν_6	1204.3	1195.3	1192.9
		1199.4	1197.7
ν_7	548.3	553.5	548.1
			548.3
ν_8	2980.4	2994.5	2985.7
ν_9	≈1447	1406.3[a]	1406[a]
ν_{10}	787	781.2	781.3
ν_{11}	149.9		
ν_{12}	≈2980	2950.2	2948.3
ν_{13}	≈1447	1444[a]	1443.8[a]
ν_{14}			698.6
			702.3
	Combination Bands		
$\nu_2 + \nu_6$	2381.8	2372.8	2367
		2373.7	2370
$\nu_{10} + \nu_{14}$	1469.8	1474.4	1474.13
$\nu_9 + \nu_{13}$	2836	2834.9	2834.4
$\nu_{13} + \nu_{10} + \nu_7$		2773.4	2773.3
$\nu_3 + \nu_{11}$		675	676.0
			678.1
			680.5
			681.6
$\nu_3 + \nu_7$	1064.8	1076.9	1065.6
$\nu_3 + \nu_6$	1724.2	1725.6	1718.4

[a] Seen only in dimers, although $\nu_9 + \nu_{13}$ is seen in monomers.

To identify the observed spectra, we recorded in addition absorption and emission spectra of Ar matrixes containing Hg atoms with controlled amounts of different hydrocarbons; spectra after laser excitation of these mixed matrixes were also observed and gave information on the photochemistry of Hg with the different hydrocarbons.

Results and Discussion

(1) On Deposition. In matrixes, no UV absorption was detected for $Hg(CH_3)_2$ in the 220−260 nm spectral range where the red wing of the gas-phase A ← X absorption band is observed. The extent of the matrix blue shift is not known but absorption at the 248 nm KrF laser wavelength does occur and is strong enough to induce dissociation. In the gas phase the ratio of absorption coefficients at the wavelengths of the KrF and ArF laser outputs $\epsilon^{248}/\epsilon^{193}$ is of the order of 1/80.[9] The value of this ratio in the matrix is not known, but it is expected to be much less than that of the gas phase if a blue shift is present.

The infrared spectra are recorded in argon at 12 K and also in nitrogen matrixes in order to get better assignments; line wavenumbers are given in Table 1. They are significantly different from those of ref 16, the discrepancy being probably due to the presence of aggregates in the samples prepared by these authors. The assignments are made by comparison with those previously proposed by Coats et al.[13] for the gas-phase spectra, the frequencies observed in argon matrixes being not very different from those in the gas.

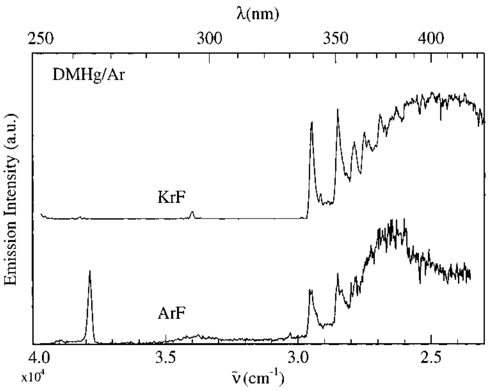

Figure 1. Comparison of the emission spectra recorded at 14 K immediately with ArF (bottom) and KrF (top) excimer laser excitation of 1/1000 $Hg(CH_3)_2$/Ar samples.

The new matrix-IR observations made may be summarized as follows. Bands corresponding to the parallel vibrations (ν_5, ν_6, ν_7) are sharper than those corresponding to the perpendicular ones, an observation previously made in the spectra of matrix-isolated dimethylzinc.[10b] In the nitrogen matrixes these bands are still narrower and split into two or more components. The bands corresponding to the ν_9 and ν_{13} modes, which are not observed in dilute (1:2000) samples, appear in more concentrated (1:1000) ones. This difference cannot be explained by their low intensities and must be due to a lower site symmetry (dimer formation) in the latter case. The case of the ν_{14} mode is similar; this line is not observed in argon matrixes but only at high (1:500) concentration in the nitrogen host. In contrast, the $\nu_9 + \nu_{13}$ combination band is fairly strong, exhibiting an intensity proportional to the concentration of the guest. A strong line at 2950 cm^{-1}, not reported by previous authors, is assigned to the ν_{12} mode. It seems surprising that this line has not been observed previously, perhaps because of the congestion of the gas-phase spectrum or because of its intensity, low in an isolated molecule and enhanced in the argon lattice. The assignments of combination bands are the same as previously proposed, with the exception of the 2773 cm^{-1} line, which cannot be a hot band[13] and is tentatively assigned to $\nu_7 + \nu_{10} + \nu_{13}$ combination band. A very weak band at 522.9 cm^{-1} appearing only in the nitrogen matrix may be assigned to the IR forbidden but Raman active ν_3 Hg−C symmetric stretching, weakly allowed by perturbation in the nitrogen lattice, which is more rigid than that of solid argon.

(2) Emission during the Irradiation of the Sample. The spectra shown in Figure 1 present the emission observed during the early stages of KrF (top) and ArF (bottom) laser irradiation. The common feature of the two spectra is the system of narrow bands in the near-UV region with the origin at 338.8 nm (29 515 ± 20 cm^{-1}) and with a decay time of a few milliseconds. The intensity of this system decreases after longer irradiation with the appearance of a new, broad, and structureless emission band with $\lambda_{max} \approx 380$ nm (25 600 cm^{-1}) and a much shorter lifetime of ~100 μs. This 380 nm emission was previously observed and assigned to the $A0_g^{\pm} \rightarrow X0^+{}_g$ emission of Hg_2 molecules formed by aggregation of Hg atoms upon a strong laser irradiation of matrixes.[18] Its high intensity is due to the efficient pumping of $G0^+{}_u$ and $F0^+{}_u$ states of Hg_2 by the 193 and 248 nm laser lines.

The assignment of the 338 nm band system is not clear. A narrow-band emission strongly red shifted with respect to Hg $^3P_1$ and $^3P_0$ levels ($\Delta\nu \approx 10\,000$ cm^{-1}) with a few millisecond lifetime was never observed for any of the Hg•X systems studied in matrixes. Two types of emission spectra have been previously recorded for the Hg•X systems. The first is a structured $^3P_0 \rightarrow {}^1S_0$ emission in the 36 000−39 000 cm^{-1} spectral region of weakly bound complexes such as $Hg{\bullet}CH_4$;[19] the second is a broad, structureless emission in the 30 000−34 000 cm^{-1} range due to exciplexes (e.g., $Hg{\bullet}N_2$ or $Hg{\bullet}NH_3$).[18]

Three types of systems can a priori be considered as responsible for the structured 338 nm emission system: (a) the $HgCH_3$ radical, (b) specific, strongly bonded complexes such as $Hg{\bullet}C_2H_4$ and $Hg{\bullet}C_2H_2$ (Hg interacting with secondary reaction products), or (c) dimethylmercury itself.

In contrast to $ZnCH_3$ and $CdCH_3$, the $HgCH_3$ radical was never observed in gas-phase experiments, probably because of its extremely low binding energy of the order 5 kcal/mol (~1750 cm^{-1}).[1] The vibrational energy excess at the first step of the $Hg(CH_3)_2 + h\nu \rightarrow HgCH_3 + CH_3$ reaction is large enough to induce dissociation of $HgCH_3$ in the gas, but it may be stabilized in the matrix. There are, however, two strong arguments against this assignment: (1) The spectral range of this emission ($\nu_0 \approx$ 29 500 cm^{-1}) is quite different from that of $ZnCH_3$ ($\nu_0 = 23\,950$ cm^{-1}), $CdCH_3$ ($\nu_0 = 22\,507$ cm^{-1}),[3,6] and HgH ($\nu_0 = 24\,932$ cm^{-1}),[20] and (2) the long (~4 ms) decay time characteristic for Hg ($^3P_0$) complexes is not expected for MCH_3 radicals.

In our attempts to identify the species responsible for the structured emission we checked for fluorescence with laser excitation of Hg in ethylene (acetylene) or mixed C_2H_4/Ar (C_2H_2/Ar) matrixes. No structured emission was observed in these samples so we conclude that the $Hg{\bullet}C_2H_4$ and $Hg{\bullet}C_2H_2$ systems are not the source of the 338 nm emission.

Another photolysis product which might be responsible for the emission is the $Hg(^3P_0){\bullet}CH_3$ complex, i.e., a mercury atom interacting with a methyl radical and not the methylmercury radical $Hg{-}CH_3$. Except the possibility of impurities in the matrix, we can propose a tentative assignment to the $Hg(^3P_0){\bullet}CH_3$ complex (and not radical), in which the formation of the Hg−C bond is hindered by steric effects. Such an assignment is consistent with its long lifetime. However, the large Stokes shift, the vibrational spacings, and the decreasing intensity of the structured emission with photolysis time indicate that this assignment is not definitive.

One possibility which has also to be considered is that the structured 338 nm system is a triplet to ground singlet state transition of the parent molecule $Hg(CH_3)_2$. Supporting evidence is (a) the long lifetime and (b) the correct photolysis-time behavior, but the match of the spacing of the structured emission and the vibrational frequencies of ground-state $Hg(CH_3)_2$ is only approximative. The spacing between the most pronounced features in the 338 nm system is 1000 cm^{-1}, which corresponds roughly to the CH_3 deformation modes recorded at 1100 cm^{-1} in IR studies of ground-state $Hg(CH_3)_2$.

Upon ArF irradiation, there are a few lines which can be assigned to emission of Hg atoms from the $^3P_2$, $^3P_1$, and $^3P_0$ states: a weak, long-lived emission at 43 500 cm^{-1}, a very weak, short-lived one at 39 000 cm^{-1}, and a strong one at 37 860 cm^{-1} with a very long (>400 ms) decay time; these transitions have been observed in pure Ar matrixes at 44 550, 39 850, and 38 650 cm^{-1}, respectively, upon excitation of autoionized atomic states.[21] The strong red-shifted bands observed here indicate that these emissions are coming from Hg atoms in perturbed environments. This is confirmed by annealing experiments in which the strong band is shifted to 38 600 cm^{-1} and broadened after annealing the sample at 25 K.

What is the origin of these atomic emissions? It has been shown[3,6] that the atomic emission of Cd and Zn upon UV irradiation of $Cd(CH_3)_2$ or $Zn(CH_3)_2$ is induced by a two-photon absorption. Also in the case of Hg, two-photon transitions seem to be the only mechanism able to populate the ^3P_i levels after excitation of $Hg(CH_3)_2$. Since the energy required for dissociation of $Hg(CH_3)_2$ into three particles is $D = 20\,600$ cm^{-1},[9] we have $D + E_i \gg h\nu_{193} = 51\,800$ cm^{-1}, where E_i is the energy of the ^3P_i state.

On the other hand, $2h\nu_{193} \gg D + I_{Hg} = 95\,100$ cm^{-1}; the two-photon excitation by an ArF laser can transfer the system into the ionization continuum with the energy excess sufficient to dissociate the $Hg(CH_3)_2^+$ ion:

$$Hg(CH_3)_2 + 2h\nu_{193} \rightarrow Hg(CH_3)_2^+ \rightarrow Hg^+ + 2CH_3 + e \rightarrow Hg^* + 2CH_3$$

the $Hg^+ + e$ recombination yielding in rare gas matrixes a strong emission from the Hg 6P levels.[21] There are, however, two experimental results in contradiction with this explanation: (i) The intensity of the 37 860 cm^{-1} band is approximately linearly dependent on the ArF laser intensity; (ii) this band is always observed after a long irradiation of the sample, i.e., when almost all the dimethylmercury is dissociated. On the other hand, we have thoroughly checked that these emissions are not excited upon the irradiation of Ar matrixes containing Hg atoms by the ArF laser. This is not surprising because of the large discrepancy between the laser energy (51 800 cm^{-1}) and the nearest atomic state of mercury ($^1P_1$ level at 56 100 cm^{-1} in Ar matrixes). So, we suggest that these emissions are coming from Hg atoms in extremely perturbed sites created in the dissociation process.

Upon KrF excitation, atomic emissions are weak. Few bands corresponding to the $^3P_0 \rightarrow {}^1S_0$ transition are observed at 38 600, 38 200, and 37 860 cm^{-1}. As Hg atoms coming from the dissociation are directly excited by the KrF laser and are emitting, these emission could come from different excited systems ($Hg(CH_3)_2^*$ or Hg^*). From the previous results, they are assigned to mercury in different, more or less perturbed sites. Nevertheless, it is sure that the intensities of Hg 6P emission upon ArF are much stronger than upon KrF excitation of the sample. This may be due either to the weak absorption of $Hg(CH_3)_2$ in the 248 nm range populating the intermediate (A) state or to a different relaxation path from the electronic states attained by two 248 nm photons.

(3) Absorption and Emission Spectra of Irradiated Samples. After ArF irradiation, the IR and UV spectra show the presence of photodissociation products.

In the UV absorption spectrum, a strong absorption band builds up at 40 550 cm^{-1}, close to the $^1S_0 \rightarrow {}^3P_1$ transition of Hg in a pure argon matrix with a slight (~100 cm^{-1}) red shift and a strongly developed red wing (Figure 2). Such spectra are characteristic of mixed matrixes having a guest molecule in the first solvation shell surrounding the Hg atom, but their shapes and the spectra of the prompt $^3P_1 \rightarrow {}^1S_0$ emission are not strongly dependent on the nature of the impurity. In contrast, the spectra of the long-lived $^3P_0 \rightarrow {}^1S_0$ emission in matrixes containing at least one molecule such as CH_4, CD_4, CF_4, or SF_6 as the nearest-neighbor of Hg show a vibrational structure involving the nontotally symmetric modes of the molecule.[19] As shown in Figure 3a, the spectra of the long-lived emission excited at different frequencies within the 40 550 cm^{-1} absorption band, especially within the low frequency wing, show a vibrational structure similar to but not identical with any of the previously studied systems.

To check its origin, we recorded absorption and emission spectra of Hg in mixed matrixes containing a few percent of C_2H_6, C_2H_4, and C_2H_2 in argon. No emission was observed from Hg/C_2H_4 and Hg/C_2H_2 centers but the emission of Hg in a mixed matrix containing 2% of ethane (Figure 3b) is practically identical with that of $Hg(CH_3)_2$/Ar samples irradiated with the 193 nm light (Figure 3a). In both cases, the spectral intervals (1470 and 3000 cm^{-1}) agree—within the error limits—with vibrational frequencies of ethane. The further confirmation of this assignment is obtained by recording the Hg emission spectra in Ar matrixes containing 2% of C_2D_6 where spectral intervals observed (1020 and 2170 cm^{-1}) agree with those of deuterated ethane (Figure 3c).

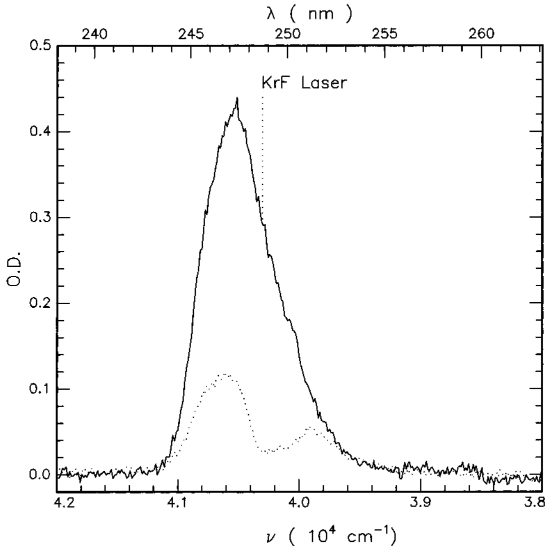

Figure 2. Absorption spectra in the Hg ($^1S_0 \rightarrow {}^3P_1$) transition spectral range: 1/1000 $Hg(CH_3)_2$/Ar sample irradiated by the ArF laser (full line); same sample subsequently irradiated by KrF laser (dotted line).

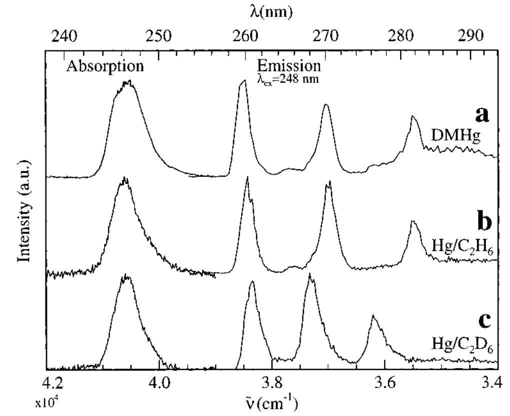

Figure 3. Absorption and emission with a dye laser excitation at 248 nm from different samples: (a) 1/1000 dimethylmercury in argon after 30 min ArF irradiation; (b) Hg/C_2H_6/Ar (0.1/1/1000); (c) Hg/C_2D_6/Ar (0.1/1/1000).

The IR spectra confirm this assignment. As shown in Figure 4b, new lines are observed in the spectral regions corresponding to the ν_8, ν_6, and ν_9 modes of ethane. The number of lines is larger than in the IR spectra of ethane in argon matrixes (Figure 4a). This suggests that some of them occupy specific sites, in the close neighborhood of Hg atoms, in good agreement with the UV data.

We can conclude, therefore, that photodissociation of $Hg(CH_3)_2$ is followed by recombination of methyl radicals:

$$Hg(CH_3)_2 + h\nu_{193} \rightarrow Hg(^1S_0) + 2CH_3 \rightarrow Hg(^1S_0) + C_2H_6$$

and that an important fraction of ethane molecules remains in

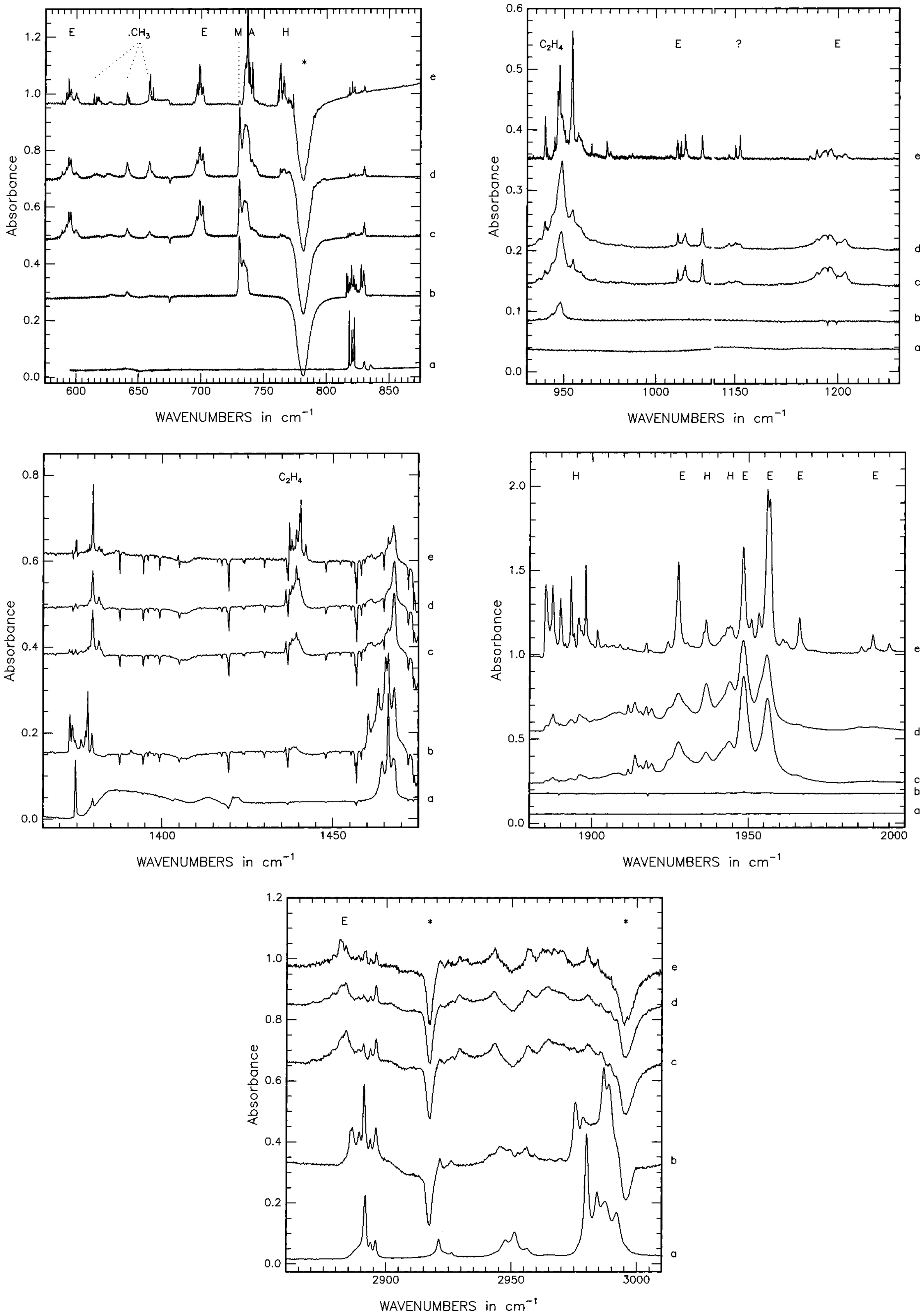

Figure 4. (a) C_2H_6/Ar 1/1000 deposited at 25 K, spectrum at 12 K, 0.8 mmol. (b)−(e) Dimethylmercury/Ar (1/2500) sample deposited at 12 K, spectra at 12 K, 8 mmol. Difference spectra (the reference spectrum is dimethylmercury before irradiation shown by *). Symbols: H for HgH_2, E for C_2H_5HgH, A for acetylene, M for CH_3...Hg. (b) After irradiation, 18 000 pulses, with a 2 mJ ArF laser (193 nm). (c) Sample (b) irradiated further with a KrF laser (750 pulses, 6 mJ). (d) Sample (c) irradiated with 3000 more KrF pulses. (e) Sample (d) after 15 min annealing at 34 K.

the close vicinity of the Hg atoms. The IR spectra show weak absorption due to C_2H_4 and traces of CH_3 radicals isolated or close to Hg (Figure 4b, Table 2). From the intensity measurements, the IR spectra show that in a 2.5×10^{-4} concentration

TABLE 2[a]

Wavenumbers (cm^{-1}) Observed after ArF Irradiation (Figure 4b)

C_2H_6 (before annealing)
816.15, 817.08, 818.26, 818.96, **819.93**, 821.86, 823.61, **827.64**, **829.62**
1372.81, 1373.59, 1374.59, 1376.19, 1377.55, **1378.14**, 1379.4
1460.3, 1463.3, **1465.4**, 1466.2, 1467.9
2886.5, 2889.1, **2891.2**, 2893.6, 2895.9
2975.4, 2978.5, **2986.7**, 2988.9

Wavenumbers (cm^{-1}) Observed after ArF and KrF Irradiation and Annealing (Figure 4e)

C_2H_6	C_2H_5HgH	CH_3 radical	C_2H_2	HgH_2 perturbed	C_2H_4 perturbed
818.22, **820.41**, 822.43, 830.32 1374.6, **1379.6** **1467.7**	588.56, 592.0, **593.87**, **595.59**, 599.7 601.9, 696.55, **698.50**, 698.94, 701.38 1013.6, 1016.0, 1025.1 1186.5, 1189.84, 1195 1203, 1233.4, 1234.2, 1242.5 **1927.63**, 1948.4, 1956.06, **1956.89**, 1966.30 **2881.4**	**614.05**, 616.26, 617.36, 618.03, 619.20, 619.60 640, **640.6**, 641.26, 642.38, 658.35, **659.28**, 661.48 CH_3 radical perturbed by Hg: **730.6**	735.3, **736.9**, 738.6, 740.9 **3285.5**, **3289.1**, 3310.1	**763.3**, 766.0, 770.6, 775.9 **1885**, 1887.25, 1889.80, 1893.26, 1895.60, **1898.0** 1901.76, 1924.32, 1936.6, 1943.3 tentatively assigned to very perturbed HgH_2: 1986.0, 1989.8, 1995.0	939.80, 946.70, 947.70, **954.72** 1437.22, 1437.93, 1439.23, 1439.96, 1440.15, 1440.31, **1440.56**, 1442

[a] Bold values correspond to the strongest absorption bands.

sample, 18 000 ArF laser pulses (2 mJ) achieved the dissociation of 95% of the dimethylmercury. Comparing the intensity of the C_2H_6 produced in the reaction (Figure 4b) to the IR absorption intensity of a known sample of C_2H_6 in argon (Figure 4a), one can deduce that around 81% of the dimethylmercury dissociates giving ethane. That means that around 20% of the methyl radicals do not recombine, probably because they are ejected from the first solvation shell after the dissociation reaction. The sharp peak at 730.6 cm^{-1} may be assigned to CH_3 radical close to a metal atom,[22,23] here mercury; this peak has an intensity almost the same as those of the two peaks around 620 cm^{-1}. The latter lines close to that of isolated methyl radical in argon matrixes, but setting at a little higher frequency, may be assigned to CH_3 radicals perturbed by mercury in the second or third shell. The broad structure at 736 cm^{-1} and two broad structures around 3270 cm^{-1} may be assigned to C_2H_2 which comes from the decomposition of C_2H_4. The formation of acetylene has been observed in a separate experiment with C_2H_4 irradiated with ArF without mercury. In contrast, C_2H_4 irradiated by KrF without mercury does not show any photochemistry. With mercury, KrF does not give any product in a C_2H_4/Ar matrix, but the local rise in temperature makes holes in it.

Upon direct KrF irradiation, no products are detected in IR, and in addition, only weak UV emission is observed with this excitation. Taking these two observations, it seems reasonable to think that photodissociation by the KrF excitation is mainly a two-photon process. When the irradiation is strong, the UV absorption spectra show in the Hg $^1S_0 \rightarrow {}^3P_1$ spectral range a much weaker absorption band with a central minimum and a peculiar asymmetric shape. Its origin may be easily understood if this spectrum is compared with that obtained by the ArF irradiation of the sample, followed by the KrF irradiation (Figure 2). The KrF laser burns a deep and broad ($\delta\nu \approx 300$ cm^{-1}) hole in the red wing of the absorption band. As evidenced by the emission spectra, the remaining part of the absorption band corresponds in its high-frequency part to Hg in pure Ar environment (C_2H_6 expelled from the first solvation shell of Hg) and to perturbed sites (Hg_2, $Hg\cdot H_2O$, defects, etc.) in its red wing.

The mechanism of this secondary photochemical reaction may be deduced from the IR absorption spectra of samples submitted first to ArF and then to KrF photolysis (see Figure 4c,d). The wavenumbers of the products are listed in Table 2.

The lines in the 1880−1960 cm^{-1} region may be assigned to the HgH stretching mode of the X−Hg−H molecules. The nature of X is more difficult to assign. Most of the lines can be assigned to $H{-}Hg{-}C_2H_5$, but the narrow lines in the 1885−1900 cm^{-1} region, which become nicely resolved with annealing, are certainly due to HgH_2. The associated bending mode of this molecule in argon (at 770 cm^{-1}) coincides with the strong absorption of the parent molecule, but the sharp peaks in the 760−770 cm^{-1} region show the same annealing behavior and are likely to be this mode. The assignment of the 1955 cm^{-1} lines to the molecule $H{-}Hg{-}CH_3$ previously observed [24] is not confirmed by observation of a line at 530 cm^{-1}, so that we think that the main product is the ethyl hydride mercury. We do notice also that the weak line assigned to CH_3 radical close to mercury (730 cm^{-1}), observed under ArF irradiation, increases slightly under KrF irradiation and decrease strongly upon annealing at 34K (Figure 4e); at the same time the lines assigned to CH_3 radical increase. In the 1900 cm^{-1} region, the difference between spectra in Figure 4c (5 min KrF) and 4d (20 min KrF) and the spectrum after annealing (Figure 4e) allows the assignment of some lines to C_2H_5HgH and the others to HgH_2, the first ones decrease under longer irradiation (Figure 4d) the second ones increase.

The main channel of the secondary reaction is then the insertion of Hg in the CH bond of ethane:

$$Hg(^1S_0)\cdot C_2H_6 + h\nu_{248} \rightarrow Hg^*(^3P_1)\cdot C_2H_6 \rightarrow H{-}Hg{-}C_2H_5$$

followed upon further irradiation by photodissociation of the ethylmercury hydride yielding ethylene and HgH_2 (and small quantities of acetylene):

$$H{-}Hg{-}C_2H_5 + h\nu_{248} \rightarrow HgH_2 + C_2H_4 \text{ or } Hg + H_2 + C_2H_4$$

as evidenced by IR spectra of irradiated samples. The same reaction takes place when Hg in ethane or in mixed Hg/C_2H_6/Ar matrixes is excited to the $^3P_1$ state by the KrF laser.

Conclusions

The photodissociation of dimethylmercury is a much more efficient process upon ArF than KrF excimer laser irradiation.

When irradiated at 193 nm in Ar, the widely predominant reaction is

$$Hg(CH_3)_2 + h\nu_{193} \rightarrow Hg(^1S_0) + 2CH_3 \rightarrow Hg(^1S_0) + C_2H_6$$

leading to a large number of sites where Hg and ethane are close to each other. In the case of the 248 nm irradiation, a very efficient secondary process,

$$Hg(^1S_0)\cdot C_2H_6 + h\nu_{248} \rightarrow Hg^*(^3P_1)\cdot C_2H_6 \rightarrow H{-}Hg{-}C_2H_5 \rightarrow HgH_2 + C_2H_4$$

has been observed upon the sequential irradiation by ArF and KrF of the dimethylmercury doped samples. Experiments on the photodissociation of dimethylmercury conducted in N_2 matrixes have given similar results to those presented here for Ar matrixes.

Acknowledgment. We thank Dr. C. Reynaud who lent us an excimer laser for the last experiments. J.M.C. gratefully acknowledges receipt of a France-Ireland Forbairt/CNRS exchange scheme grant in 1995 and the Royal Irish Academy for one in 1997.

References and Notes

(1) Chen, C. J.; Osgood, R. M. *J. Chem. Phys*. **1984**, *81*, 327.
(2) Ibuki, T.; Hiraya, A.; Shobatake, K.*J. Chem. Phys*. **1990**, *92*, 2797.
(3) Amirav, A.; Penner, A.; Bersohn, R. *J. Chem. Phys*. **1989**, *90*, 5232.
(4) Penner, A.; Amirav, A.; Bersohn, R. *Chem. Phys. Lett*. **1991**, *176*, 147.
(5) Jackson, R. L. *Chem. Phys. Lett*. **1990**, *174*, 53.
(6) Yu, C. F.; Youngs, F.; Tsukiyama, K.; Bersohn, R. *J. Chem. Phys*. **1986**, *85*, 1382.
(7) Kallend, A. S.; Purcell, J. H. *Trans. Faraday Soc*. **1966**, *60*, 93.
(8) Snelson, A. *J. Phys. Chem*. **1970**, *74*, 537.
(9) Baughcum, S. L.; Leone, S. R. *Chem. Phys. Lett*. **1982**, *89*, 183.
(10) (a) Bracken, V. A.; Gürtler, P.; McCaffrey, J. G. *J. Phys. Chem*. **1997**, *101*, 9854. (b) Bracken, V. A.; McCaffrey, J. G.; Legay-Sommaire, N. *J. Phys. Chem*. **1997**, *101*, 9863.
(11) Gutowsky, H. S. *J. Chem. Phys*. **1949**, *17*, 128.
(12) Butler, I. S.; Newbury, M. L. *Spectrochim. Acta*, **1977**, *33A*, 669.
(13) Coats, A. M.; McKean, D. C.; Edwards, H. G. M.; Fawcett, V. *J. Mol. Struct.* **1994**, *320*, 159.
(14) Bakke, A. M. W. *J. Mol. Spectrosc*. **1972**, *41*, 1.
(15) Kippels, C.; Thiel, W.; McKean, D. C.; Coats, A. M. *Spectrochim. Acta* **1992**, *A48*, 1067.
(16) Bochmann, M.; Chesters, M. A.; Coleman, A. P.; Grinter, R.; Linder, D. R. *Spectrochim. Acta* **1992**, *A48*, 1173.
(17) (a) Legay-Sommaire, N.; Legay, F. *Chem. Phys. Lett*. **1993**, *207*, 123. (b) Legay-Sommaire, N.; Legay, F. *J. Phys. Chem*. **1995**, *99*, 16945.
(18) Crépin, C.; Tramer, A. *J. Chem. Phys*. **1994**, *100*, 5475.
(19) Crépin, C.; Tramer, A. *J. Chem. Phys*. **1997**, *107*, 2205.
(20) Herzberg, G. Molecular spectra and molecular structure I. *Spectra of Diatomic Molecules*; van Nostrand: New York, 1950.
(21) Chergui, M.; Crépin, C.; Hebert, T.; Tramer, A. *Chem. Phys. Lett*. **1992**, *197*, 467.
(22) Tan, L. Y.; Pimentel, G. C. *J. Chem. Phys*. **1968**, *48*, 5202.
(23) Andrews, L.; Pimentel, G. C. *J. Chem. Phys*. **1967**, *47*, 3637.
(24) Legay-Sommaire, N.; Legay, F. *Chem. Phys. Lett*. **1994**, *217*, 97.